National Aeronautics and
Space Administration

Report Number: 20230013923
Revision: Basic
Effective Date: 09/30/2023

Center Innovation Fund (CIF) Project

Passively Cooled Superconductors Final Report

Mark A. Nurge, Tracy Gibson, Madeleine DeFillipo, Chris Biagi, Nick Spangler, and Annelisa Esparza

Background

A highly reflective spray-on coating and tile material has been under development at Kennedy Space Center (KSC) that scatters away most of the Sun's energy, thereby allowing coated objects to remain cool in space. The best performing tile material has achieved 1% solar absorptivity while the best performing spray-on coating has achieved around 4%. Both versions passively maintain cryogenic temperatures below 120 K at 1 astronomical unit (AU) from the Sun, but the tile material consistently sustains temperatures below 90 K, which is low enough to preserve oxygen and methane in a liquid state.

Besides keeping propellants cold, this "solar white" material has the potential to passively maintain high-temperature superconductors (HTS) in a superconducting state without the support of liquid nitrogen cooling. If superconductors can be operated without the added infrastructure of liquid nitrogen cooling, it may enable them to be used in space for applications like magnetic radiation shielding and efficient energy management. Long duration exposure to both galactic cosmic radiation and coronal mass ejections can pose health risks for the astronauts and increase the potential for damage to electronics. This makes shielding essential to accomplish long duration missions, particularly when astronauts are onboard.

The objective of this project was to determine the extent we could keep a high-temperature superconducting (HTS) material passively chilled to maintain its superconducting state. Both the tile and spray-on versions of solar white were investigated. We focused on finding a version that could support passive cooling at 1 AU from the Sun and determined the closest operating distances for samples that were unable to perform at 1 AU. Early in the project, we selected bismuth strontium calcium copper oxide (BSCCO) as the HTS to test based on its reputable usage in superconducting wires. The version we selected was Bi-2223, which has a critical temperature of about 108 K. Sample bars with contacts for a four-point probe were obtained from Quantum Levitation: https://quantumlevitation.com/product/superconductor-bar-for-4-point-tc-experiment/.

Testing was performed in the deep space simulator developed by the Cryogenics Test Lab at Kennedy Space Center, by subjecting samples to the cold temperatures of space while only in the presence of the Sun. The test chamber was evacuated and then chilled to below 20 K by a cryostat with a cold head. The cold head has a sample chamber made of copper and painted flat black on the interior. Samples smaller than approximately 2" across were suspended by Kevlar string to isolate radiation as the primary mechanism for heat transfer.

Testing with Spray-on Solar White on Cast Aluminum

A 1.5 inch diameter (37.4 mm) aluminum sphere (ADC12/A383) had pockets machined into it as shown in Figure 1 to house the HTS sample along with a silicon diode temperature sensor from Scientific Instruments (https://www.scientificinstruments.com/cryogenic-temperature-sensors/). Stainless steel screws were used to attach and suspend the sphere in the test chamber. Each HTS bar is about an inch long and has a mass of 1.468 g with the 36-gauge wire attached. The sample was wrapped in Kapton tape as seen in Figure 2 to keep it from shorting via contact with the aluminum sphere. Figure 3 shows the sphere with the HTS bar and Si-diode installed and held in place with a special varnish designed for low temperature use. The final assembly used in testing

is shown in Figure 4. The sphere was coated with 15 layers of our yttrium oxide/potassium bromide paint while in the fixture to minimize handling and contamination.

Figure 1: 37.4mm diameter aluminum sphere (ADC12/A383) with pocket for the HTS and the silicon diode temperature sensor. The stainless-steel screws are for mounting and suspending the sphere in the deep space simulator.

Figure 2: BSCCO 2223 HTS sample with 36-gauge wire attached for a four-point resistance measurement to monitor the superconductor transition. The HTS has been wrapped in Kapton tape to prevent electrical contact with the aluminum sphere.

Figure 3: Aluminum sphere with the HTS sample and the silicon diode temperature sensor inserted and secured with a low temperature varnish.

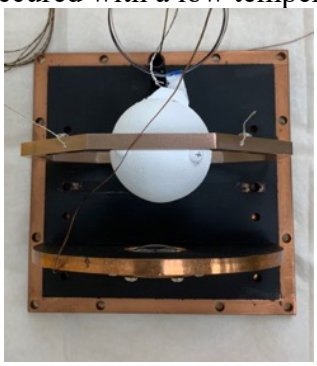

Figure 4: Photo showing the fully assembled and coated sphere suspended from the ring that is inserted into the deep space simulator.

A dental light source with a xenon bulb was used with a UV-grade fused silica fiber bundle to transmit the light to the test chamber. Inside the chamber, a lens made from similar material was used to focus the light into a 20 mm diameter spot on the test object. The light's power output was measured with a Thorlabs PM400 meter and an S425C thermal power sensor. The measured output was 1.168 W, but this needed to be adjusted using the overlap integral of the spectral output of the lamp, the response of the fiber, and the response of the sensor.

The actual power reaching the sample was determined to be 1.194 W. To simulate the power of light at the Earth, we should have been delivering 1.527 W of power. So, for our test conditions, we had 0.78 of the Earth equivalent power reaching the sample. Using a Stefan-Boltzmann energy balance, we computed the equilibrium temperatures for different amounts of solar absorptance by the solar white. The results in Figure 5 show that for a spherical shape at 1.13 AU (0.78 solar), the absorptivity needs to be below 2.8% to achieve the critical temperature and around 2.4% to remain in a superconducting state below 104K.

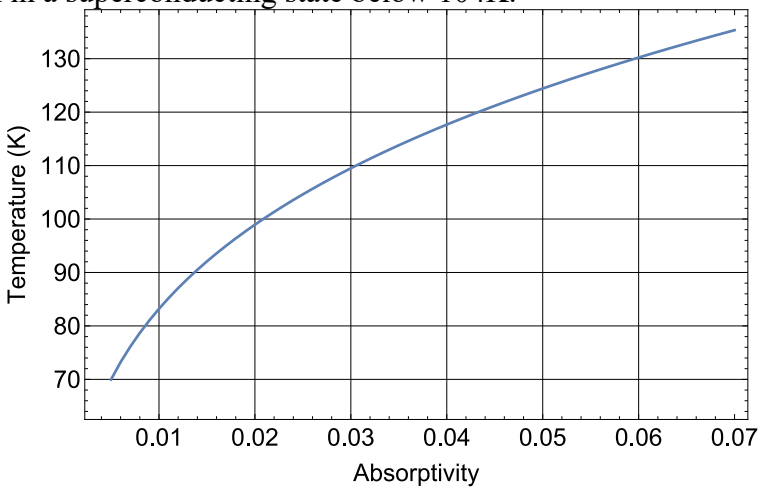

Figure 5: Plot showing the predicted equilibrium temperatures for the test sphere coated with solar white paint for different amounts of absorptivity. Emissivity is assumed (and measured) to be 1.

The superconductor resistance began falling rapidly at around 113 K to about 104 K when it reached zero. This drop in superconductor temperature took about 3 hours to complete the transition from non-superconducting to the superconducting state. This data is shown in the plots shown in Figure 6.

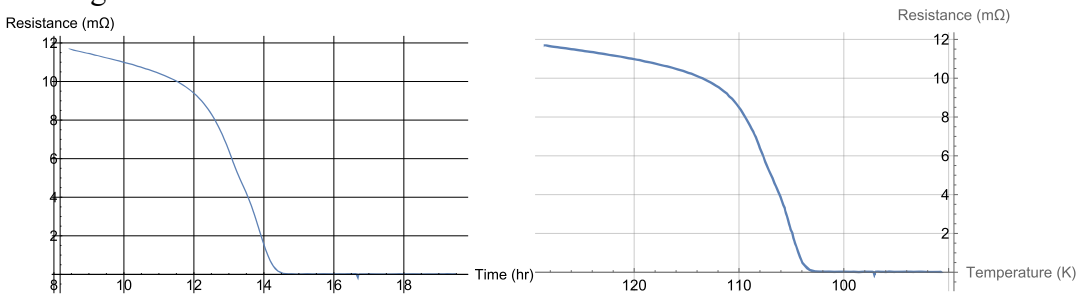

Figure 6: Plots showing the transition of the HTS to the superconducting state.

Using physical models for the components used in the experiment can write a pair of energy balance equations that computes the change in temperature for a small timestep. The equation uses the specific heat and mass of the aluminum sphere, the characteristics of solar white, the power delivered by the light source, sensor wires, and the temperature sensor. Without the light on the equation is:

$$T_{n+1} = T_n + \Delta t \frac{P_{sensor} - \sigma\epsilon A\left({T_n}^4 - {T_{Cell}}^4\right) - k\left[\frac{T_n}{2} + \frac{T_{Cell}}{2}\right]\frac{(T_n - T_{Cell})}{d}}{m c_v[T_n]},$$

where: T_n, sample temperature of timestep n

T_{n+1}, sample temperature for timestep n+1 after Δt seconds have elapsed

T_{Cell}, temperature for timestep n of the test cell/chamber

P_{sensor}, power used by the embedded temperature sensor plus the power used to measure the superconductor resistivity (1 V*10μA+100 to 350 μW =110 to 360μW)

σ, Steffan-Boltzman constant

ϵ, emissivity of the solar white coating

A, surface area of the solar white coating

$k\left[\frac{T_n}{2} + \frac{T_{Cell}}{2}\right]$, temperature dependent thermal conductivity of the phosphor bronze sensor wire and the temperature used in the average of the end temperatures

d, length of sensor wire between the sensor and the wall of the chamber

m, mass of the aluminum sphere

$c_v[T_n]$, heat capacity of aluminum at the temperature associated with timestep n

This equation was used to find the emissivity that fits the measured chill down data. An emissivity of 1 produced an excellent match to the data as shown in Figure 7 below.

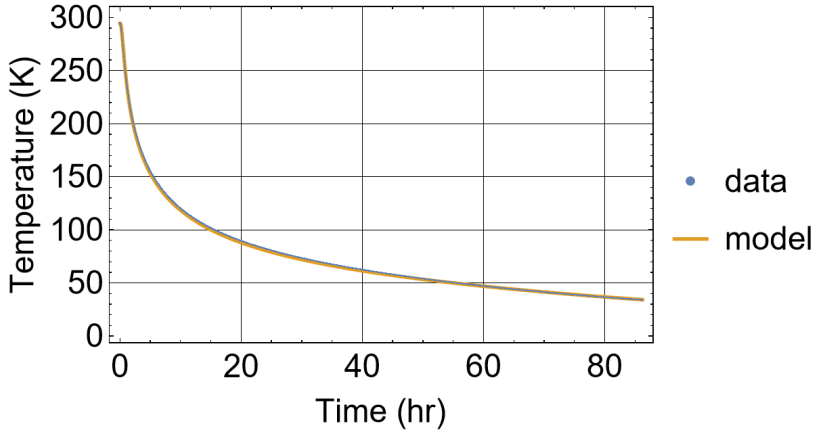

Figure 7: Plots showing the close agreement between the raw data and the model when the emissivity is set to 1.

When the light source is turned on, the equation must be modified to include the power that hits the sample times the absorptivity:

$$T_{n+1} = T_n + \Delta t \frac{\alpha P_{Source} + P_{sensor} - \sigma\epsilon A\left({T_n}^4 - {T_{Cell}}^4\right) - k\left[\frac{T_n}{2} + \frac{T_{Cell}}{2}\right]\frac{(T_n - T_{Cell})}{d}}{m c_v[T_n]},$$

where the variables are all the same as above with the addition of:

α, absorptivity of the solar white coating

P_{Source}, light source power that reaches the solar white coating

Determining the correct value to use for P_{Source} is challenging as there are several variables. A xenon bulb was used to illuminate a custom-built fiber optic cable with a fused silica core, a doped fused silica cladding, and a numeric aperture of 0.22. The end of the fiber was chilled at the point where it entered the test cell/chamber. The light output by the fiber illuminated a focusing lens made of fused quartz before projecting onto the sample. The transmission of each of these parts in the optical path is wavelength dependent and possibly temperature dependent.

At room temperature, the light at the end of the fiber optic bundle was measured as 1.168 Watts with a Thorlabs S425C thermal sensor. However, the absorptivity of the coating used in the thermal sensor needs to be compensated for in this reading. At visible wavelengths, about 91.5% of the power was absorbed by the sensor while in the infrared the absorption drops off to near 85%. To compensate for this non-linearity in the sensor and the light source, an overlap integral was done where the output is multiplied by the absorptivity at each wavelength and then summed. The results were divided by the integral of the light source output and then inverted to get a correction factor. In our case, the power reading had to be increased by about 10% (multiplied by a factor of 1.0991) to get the proper output level. The lens also reflected part of the signal due to its index of refraction. For fused silica, the transmission was assumed to be about 0.93. This resulted in about 1.194 Watts of energy illuminating the test sphere.

An earlier test to characterize the effects temperature has on the light guided by the fiber optic bundle suggested that there was a loss of 16% of the light when chilled to 20 K (Swanger, et al. 2022). However, later analysis showed that it is more likely the cladding experienced a minor reduction in its index of refraction. This would cause a change in the numeric aperture at the output and result in a reduction of the power density but not the overall power. Consequently, earlier published test results for solar white are likely to have overstated the absorptivity of the samples due to an underestimation of the irradiance through the combined optics.

For the first test with 15 layers of spray-on coating, we lost part of the data after an operator error turned the light source on during warmup. We were still able to perform an excellent fit to the data despite obtaining a rather high 6.1% solar absorbance. The data fit was extended to the captured end point and the fit remained true. This is shown in both the left and right plots of Figure 8.

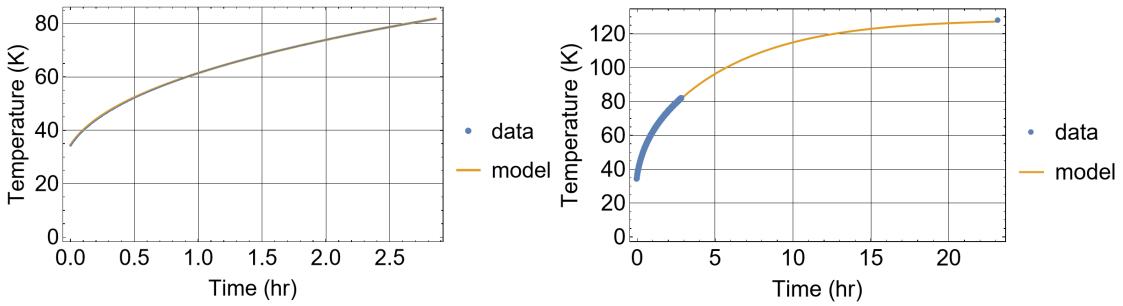

Figure 8: The plot on the left shows the data and model fit until recording accidentally stopped while the plot on the right shows the same data set with the final recorded temperature 23+ hours after the light source was turned on.

For the second test, five additional layers of the spray-on coating were added on top of the original fifteen layers. The emissivity remained at 1.0 while the absorptivity was reduced to about 5.2% for an improvement of 0.9%. The resulting fits to the data sets are shown in Figure 9. It is of note that earlier tests were performed using a highly polished aluminum alongside an uncorrected lamp output, which resulted in a 4% absorptivity. The cast aluminum sphere used in these subsequent tests had a rough, matte gray finish that does not reflect visible light as well as the earlier, mirror-like material. Longer wavelengths (i.e., IR) of light will penetrate the rather thin layers of the spray-on coating and hit the aluminum. Most metals are good reflectors in the IR and can also be good in the visible if highly polished. We are currently in the process of obtaining polished solid aluminum spheres and we will repeat this experiment to determine if there is any significant improvement. We may also experiment with the application of a thin silver topcoat layer to the sphere, as silver has almost no absorption in the visible or IR ranges.

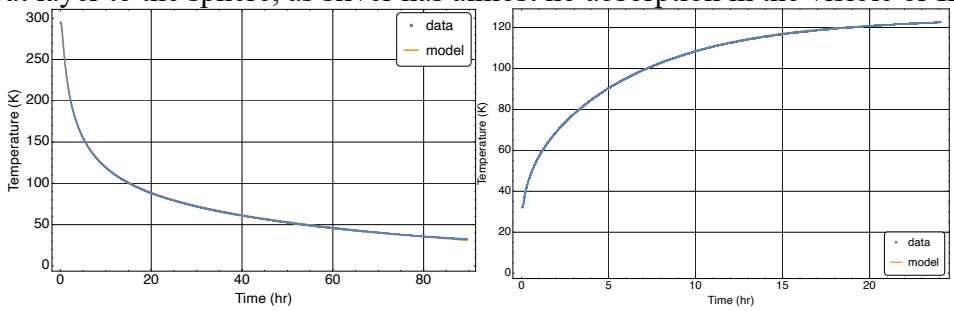

Figure 9: Plots showing the close agreement between the data and the physics model. The left plot illustrated the chill-down with the light off and an emissivity of 1.0. The right plot shows the data when the light is on where the model assumes an absorptivity of 5.25%.

Testing the Spray-on Coating with a Polished Metal Backing

The procedure was repeated with a highly polished aluminum sphere seen in Figure 10. The sphere was installed in the same test fixture shown in Figure 4 and covered with 15 layers of solar white spray-on coating. Figure 11 shows the plotted results with an emissivity of 1 and an absorptivity of 6.9%. This was a bit surprising as it was hypothesized the long wave radiation would reflect better with the polished aluminum. We decided to add ten more layers and retest.

Figure 10 – Photo of highly polished aluminum sphere with the superconductor temperature sensor installed.

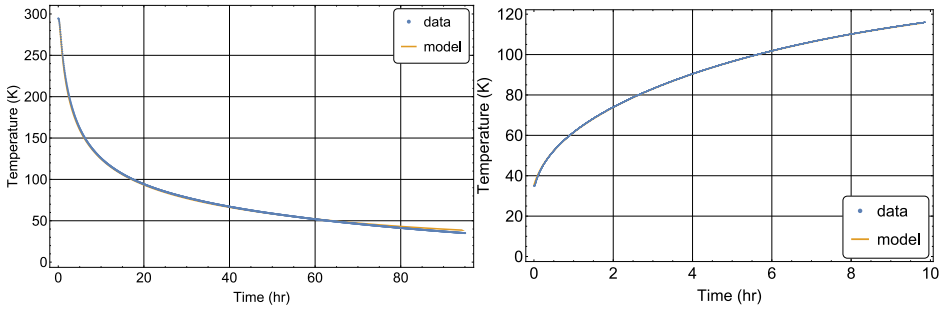

Figure 11: Plots showing the close agreement between the data and the physics model. The left plot illustrated the chill-down with the light off and an emissivity of 1.0. The right plot shows the data when the light is on where the model assumes an absorptivity of 6.9%.

Figure 12 shows the additional 10 layers resulted in an emissivity of 1 and an absorptivity of 5.1%, which was a reduction of 1.8% in absorptivity. This appears to be an important trend and it would be interesting to see if each additional 10 layers would drop the absorptivity by 1.8% until you approach the tile limit, which we've calculated to be about 1%.

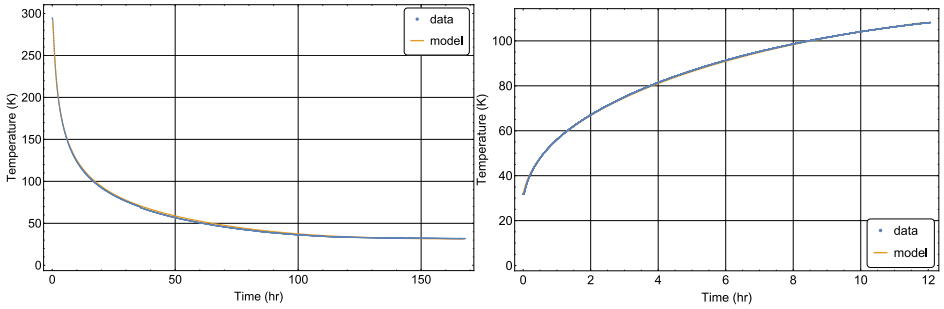

Figure 12: Plots showing the close agreement between the data and the physics model. The left plot illustrated the chill-down with the light off and an emissivity of 1.0. The right plot shows the data when the light is on where the model assumes an absorptivity of 5.1%.

An important computation was the maximum absorptivity allowable at 1 AU with a cylindrical geometry that would still passively maintain the superconductor in its superconducting state. By altering the computations for Figure 5, we can arrive at a similar curve that shows the allowable absorptivity as a function of distance from the Sun required to maintain the superconductor at 104 K . The result is shown in Figure 13 below.

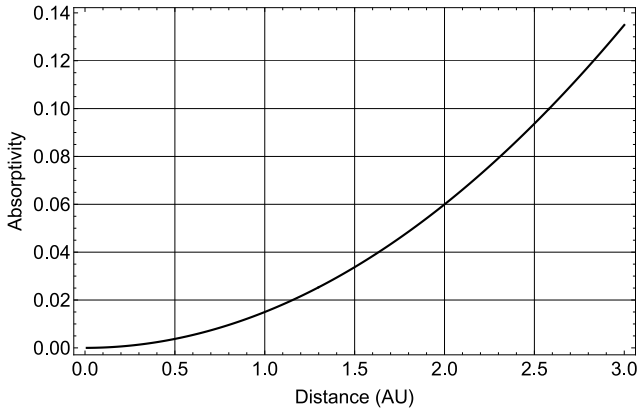

Figure 13: Plots showing the maximum allowed absorptivity as a function of distance from the Sun needed to maintain the superconductor at 104 K using a cylindrical sleeve geometry.

This plot tells us that the spray-on coating with 5.1% absorption would only work for keeping the superconductor cold enough at distances beyond 1.84 AU from the Sun. However, it does appear that adding more layers could reduce the absorption quite a bit further. Unfortunately, we were not able to explore this at present due to a compressed schedule. Tile versions of solar white have had as low as 1% absorptivity and would be capable of maintaining superconducting temperatures beyond 0.81 AU from the Sun.

Testing with Yttrium Oxide Tiles

The final set of tests was conducted with a set of three disks made from yttrium oxide following fabrication issues with barium fluoride tiles. The front disk faced the light source and was 3.0 mm thick and had a diameter of 36.7 mm and a mass of 7.543 g. The middle disk had pockets machined into it to hold the superconductor and the temperature diode. It was 3.1 mm thick, had a diameter of 36.7 mm, and a mass of 6.853 g due to the pockets. The back disk faced away from the light source and had a few small holes to pass wires through for the superconductor and the temperature sensor. It was 3.0 mm thick, had a diameter of 36.6 mm, and a mass of 7.499 g. The configuration is shown in Figure 14 below. There were three small holes to tie the disks together and mount them in the test cell. Since performance is better with a metal long-wave reflector, a piece of silver foil was inserted behind the front tile. A piece of Kapton tape was inserted behind the silver to eliminate the potential for electrical shorts between the sensors and their connections.

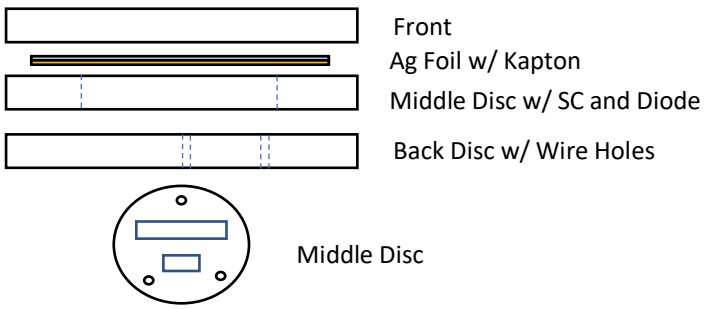

Figure 14: Configuration of yttrium oxide tiles

When mounted in the deep space simulator, the heat capacity, mass, and surface area of the Y_2O_3 tiles become the dominant physical parameters needed to model the cooling behavior. Because Y_2O_3 is an insulator, different parts of the cylinder formed by the disks will be at different temperatures and have gradients when cooling and heating once the light source is turned on. The temperature sensor reached around 86 K when the superconductor switched to the superconducting state, which we know occurs at 104 K. Ultimately, the entire sample will reach the equilibrium temperature with no heat sources. Figure 15 shows the curve of the superconductor's predicted cooling along with the curve for the embedded temperature sensor. The formula used for the temperature dependent heat capacity for yttrium oxide is as follows: $c_p(T) = 2.98989 \times 10^{-12} * T^6 - 3.47249 \times 10^{-9} * T^5 + 1.71232 \times 10^{-6} * T^4 - 4.48341 \times 10^{-4} * T^3 + 5.89544 \times 10^{-2} * T^2 - 1.21931 * T + 11.0242.$

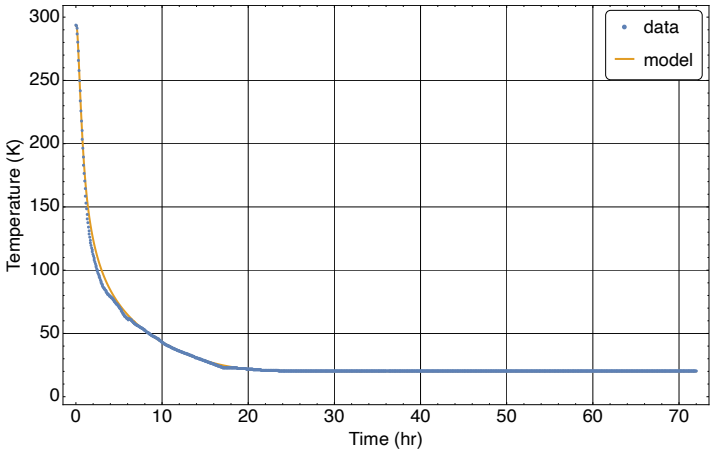

Figure 15: Blue curve showing the output of the temperature sensor cooldown in the cryostat when the light source is off. The model line shows the predicted cooldown of the superconductor. Emissivity was modeled as 1.0.

If we assume that the superconductor still goes superconducting at around 104 K, we may adjust the absorption figure until we get a crossover at that temperature. The predicted temperature curve along with the temperature sensor output is shown in Figure 16 below. The predicted curve was generated assuming a solar absorption of 2.6%, which is higher than we've seen in recent samples.

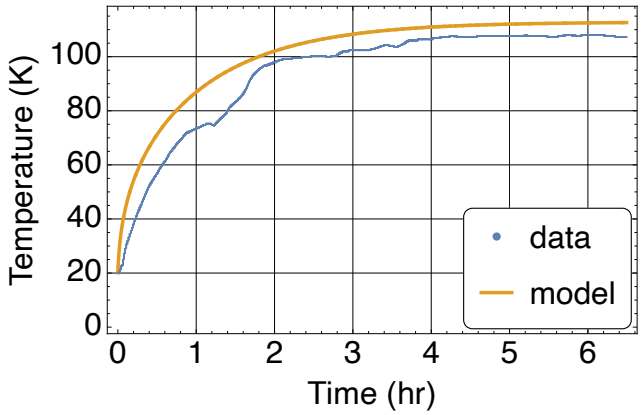

Figure 16: Plot showing the data from the temperature sensor with the light source turned on and the predicted curve for the temperature of the superconductor assuming solar absorption of 2.6%.

Besides the higher absorption, another irregularity was that the temperature sensor should have followed a smooth curve towards the equilibrium temperature. During both the chilldown and the heating cycles, the temperature sensor showed some irregular motion. One possible explanation is movement of the disks with respect to one another. However, there were no signs of broken support threads upon opening the test chamber at the end of the test. We suspect that this movement may have been due to the vibrations from the vacuum pump and cryostat cooling pump. Breaking contact between the disk faces would interrupt the conductive heat path and could also be responsible for the irregular behavior of the temperature sensor. Focusing on the tile, there is always a possibility for contamination while machining the disks and mounting the sensors and sample in the test chamber. As it stands, this solar white sample would only allow us to keep the superconductor cold beyond around 1.25 AU (from Figure 13).

Discussion/ Conclusions

The best solar white sample we have tested to date is still an order of magnitude higher in its absorptance than predicted by theory (1% vs 0.1%). The lab environment requires sharing ovens and other equipment that can cause one set of samples to vary from another. Hopefully, as the product is transitioned to commercial industry, improvements in procedure and dedicated hardware will enable them to consistently achieve absorptivities of less than 1.5% that are needed to keep BSSCO wire passively chilled at 1 AU and beyond.